CHEMPLUSCHEM
FULL PAPERS

DOI: 10.1002/cplu.201402030

Syntheses, Structures, and Luminescence Properties of Lanthanide Coordination Polymers with a Polycarboxylic Terpyridyl Derivative Ligand

Juan Xie,[a] Hui-Ming Shu,[b] Huai-Ming Hu,*[a] Zhong-Xi Han,[b] Sa-Sa Shen,[a] Fei Yuan,[a] Meng-Lin Yang,[a] Fa-Xin Dong,[a] and Gang-Lin Xue[a]

Solvothermal reactions of lanthanide chloride with a new ligand, H_3L, 4′-(3-carboxylpyridyl)-2,2′:6′,2″-terpyridine-6,6″-dicarboxylic acid, yields seven new lanthanide–organic frameworks: $\{[Ln_2L_2]\cdot H_2O\}_n$ (Ln = Pr (**1**), Nd (**2**), Sm (**3**), Eu (**4**)), $\{[Ln_5L_4(COO)_3(H_2O)_4]\cdot 10\,H_2O\}_n$ (Ln = Tb (**5**), Dy (**6**)), and $[Yb_2L_2(H_2O)_2]\cdot 2\,H_2O$ (**7**). Single-crystal X-ray diffraction reveals that these complexes belong to three structural types. Type I (**1**–**4**) consists of lanthanide–carboxyl group layers pillared by L^{3-} to form a three-dimensional network. Type II (**5** and **6**) comprises a right-handed helical chain and a left-handed helical chain linked through L^{3-} anions into a three-dimensional framework. Type III (**7**) is a discrete dinuclear structure. The structural change is due to the decrease in the metal coordination number from nine for the large ions to seven for the small ions; this demonstrates the effect of lanthanide contraction. These materials exhibit high thermal stability. In addition, the luminescent properties of these complexes are discussed.

Introduction

In recent years, the design and construction of lanthanide metal–organic frameworks (Ln-MOFs) have been extensively concerned with not only their intriguing topological structures, but also interesting photoluminescence.[1–3] Lanthanide complexes exhibit intense luminescence because of the long-lived (millisecond timescale) excited states of Ln^{III} ions.[4] Luminescence has been instrumental, and these lanthanide elements have played important roles in lighting and light conversion technologies, such as lasers, cathode-ray and plasma displays, and light-emitting diodes.[5–7] Lanthanide luminescence has been applied in material sciences. For instance, europium and terbium complexes emit fluorescence in the visible spectral region and are used as sensors and luminescent labels in fluoroimmunoassays and time-resolved microscopy.[8] Some Nd^{III} and Yb^{III} compounds, which emit in the near-infrared (NIR) region, might be good candidates for use in medical diagnostics and two-photon fluorescence imaging at longer emission wavelengths.[9]

Generally, the emissions from lanthanide metal ions are very weak.[10] One method to improve the weak luminescence properties of lanthanide ions is to use a suitable sensitizing chromophore as an "antennae" in the lanthanide metal complexes.[11] To date, many aromatic pyridine–carboxylate ligands, which are good sensitizers to stimulate lanthanide ion luminescence, have been used as chromophoric antenna ligands.[12,13] More recently, we have designed and synthesized 4′-(3-carboxylpyridyl)-2,2′:6′,2″-terpyridine-6,6″-dicarboxylic acid (H_3L; Scheme 1) as a new polycarboxylic terpyridyl derivative ligand to construct Ln-MOFs with four inherent chemical features: 1) the large conjugated system, which may act as a chromophore; b) the H_3L ligand possesses three carboxylate and four pyridyl groups, which result in multiple potential metal binding sites; c) oxygen and nitrogen atoms, as well as aromatic rings, may form hydrogen bonds and π–π stacking interactions to extend and stabilize the entire framework; and d) rotation of the C–C single bond between the two pyridyl rings, which could adapt the ligand to the coordination geometries of the metal ions.

Herein, we report the syntheses and crystal structures of seven lanthanide complexes, namely, $\{[Ln_2L_2]\cdot H_2O\}_n$ (Ln = Pr (**1**), Nd (**2**), Sm (**3**), Eu (**4**)), $\{[Ln_5L_4(COO)_3(H_2O)_4]\cdot 10\,H_2O\}_n$ (Ln = Tb (**5**), Dy (**6**)), and $[Yb_2L_2(H_2O)_2]\cdot 2\,H_2O$ (**7**). Single-crystal X-ray diffractions show that these seven compounds are of three types of structures. Moreover, the solid-state photoluminescence of **2**–**7** have been investigated at room temperature.

Results and Discussion

Synthesis

The 4′-pyridyl-2,2′:6′,2″-terpyridine ligand, which consists of four pyridyl rings, can provide a large π-electron conjugated system to absorb and transfer energy. However, because the f

---

[a] J. Xie, Prof. Dr. H.-M. Hu, S.-S. Shen, F. Yuan, M.-L. Yang, F.-X. Dong, Prof. G.-L. Xue
Key Laboratory of Synthetic and Natural Functional Molecule Chemistry of Ministry of Education, College of Chemistry and Materials Science
Northwest University, Xi'an 710069 (P. R. China)
Fax: (+86) 29-88303331
E-mail: ChemHu1@NWU.EDU.CN

[b] H.-M. Shu, Z.-X. Han
Xi'an Modern Chemistry Research Institute
Xi'an 710065 (P. R. China)

Supporting information for this article is available on the WWW under http://dx.doi.org/10.1002/cplu.201402030.

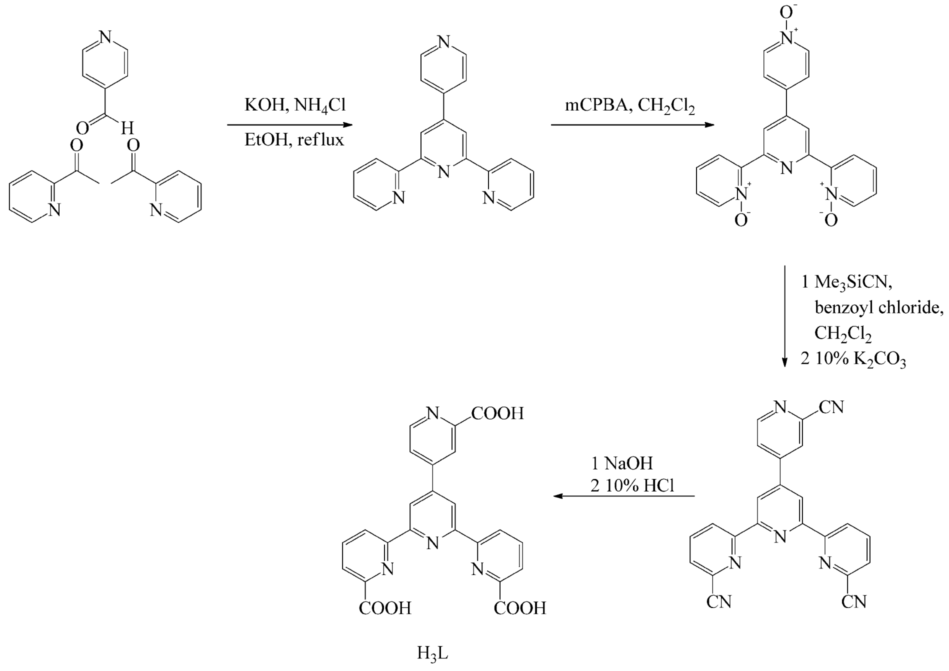

Scheme 1. Synthetic route to the ligand H_3L. mCPBA = *m*-chloroperbenzoic acid.

orbitals of lanthanides are buried, this leads to difficulties in reacting with 4-pyridyl-2,2′:6′,2″-terpyridine. A H_3L ligand that contained three carboxylate groups and four pyridyl rings, which is beneficial for the reaction of oxophilic lanthanide cations, was designed and synthesized (the synthetic route is shown in Scheme 1). In addition, if the carboxylate in the *ortho* position with respect to the nitrogen atom of pyridine generates Ln–O bonds, it is easy to form Ln–N bonds between the lanthanide cation and the pyridine nitrogen atom. Complexes **1**–**4** and **7** were prepared under solvothermal conditions (160 °C, 3 days) by the treatment of hydrated lanthanide chloride and H_3L at a molar ratio of 1:1. It is interesting to note that the synthetic methods for coordination polymers **1**–**4** and **7** are identical, apart from the lanthanide chloride, but the target products exhibit three distinct structural types: Pr^{III}, Nd^{III}, Sm^{III}, and Eu^{III} ions form a 3D structure with four ligands are around each Ln^{III} ion in **1**–**4**; Yb^{III} ions form a dinuclear structure with one ligand and one water molecule are around each Yb^{III} ion in **7**. The clearly differences in crystal structures between **1**–**4** and **7** can be ascribed to the different ionic radii of the lanthanide metals. It has long been known that DMF can be hydrolyzed into HCOOH and $(CH_3)_2NH$. Under neutral conditions, the rate of this reaction is very slow, whereas under basic or acidic conditions and high temperatures, the rate of the reaction increases dramatically. Complexes **5** and **6** are produced at higher temperature (180 °C, 3 days). The $HCOO^-$ anions appear in the construction of the crystal structure and assist L^{3-} ligands with Tb^{III} and Dy^{III} ions to form the 3D structure.

Crystal structures of 1–4 (type I)

Single-crystal X-ray analyses revealed that compounds **1**–**4** were isostructural and had three-dimensional frameworks. Here, we select **2** as the representative example for a detailed discussion of the structure. Complex **2** crystallizes in the monoclinic space group $P2_1/c$ with one Nd^{III} ion, one L^{3-} ligand, and one uncoordinated water molecule in the asymmetric unit (Figure 1 a). Each Nd^{III} ion is nonacoordinated by four nitrogen atoms (N1, N2, N3, N4A) from two L^{3-} ligands and five carboxylate oxygen atoms (O2, O3, O6A, O5B, O1D) from four L^{3-} ligands form a distorted tetrakaidecahedron coordination geometry (Figure 1 b). The Nd–O bond lengths are in the range of 2.400(2) to 2.502(2) Å. The Nd–N bond lengths of 2.605(3) and 2.774(3) Å are similar to those of previously reported Nd–N bond lengths.[14] Owing to the difference between the atomic radii of nitrogen and oxygen, the Nd–N bond lengths are longer than the Nd–O bond lengths.[15] The pyridyl rings of the L^{3-} anion are nonplanar. The N4 pyridyl ring is twisted with respect to the central pyridyl ring (N2 pyridyl) with a dihedral angle of 48.79°.

The 3D framework consists of neodymium–carboxyl group layers pillared by ligands. The neodymium–carboxylate group layers consist of [Nd(COO)] chains running along the *b* direction (Figure 1 c). Within the chain, the Nd^{III} ions are arranged in a zigzag fashion. It is important to note that there are $[Nd_2(COO)_2]$ units with two Nd–O–C–O–Nd connectivities owing to two carboxylate groups of ligands in a *syn*–*syn* bridging model (Figure S1 in the Supporting Information). The Nd–Nd distance in the $[Nd_2(CO_2)_2]$ unit is 6.0402(6) Å. These units are linked by a carboxylate group to form a zigzag-like chain along the direction of the *b* axis. The nearest Nd–Nd distance between the units along the chain is 6.3924(5) Å. These chains are linked by a bridging carboxylate to generate a two-dimensional framework. The linking of adjacent chains occurs through the binding of the carboxylate groups. The neodymium–carboxylate group layers, which are parallel to the *bc* plane, are further pillared by ligands to generate a three-dimensional framework (Figure 1 d). Each Nd^{III} ion is linked with four ligands and, in turn, each ligand is linked with four Nd^{III} ions. If the Nd^{III} cation and ligand L^{3-} anion act as four-connected nodes, the complicated architecture of **2** is simplified to a (4,4)-connected 3D topological network with the Schläfli symbol of $(4^2.6^3.8)$, as shown in Figure 1 e.

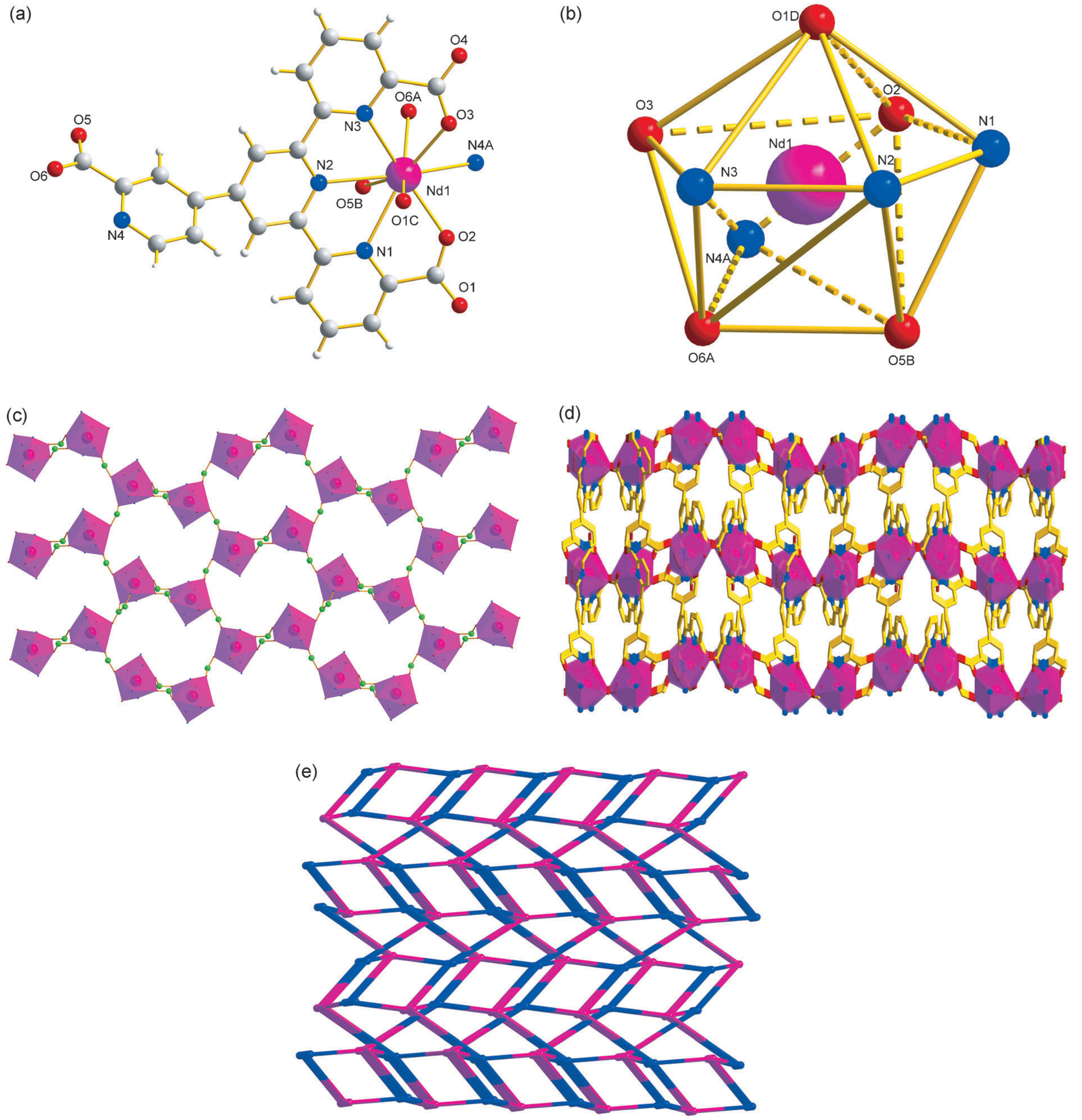

Figure 1. a) Representation of the Nd^{III} coordination environment in **2**. b) The distorted tetrakaidecahedron coordination polyhedron of Nd^{III} ion. c) A view showing that the metal chains are linked by bridging carboxylate to generate a 2D framework in **2**. d) View of the 3D network in **2**. e) View of the 3D topological network in **2**. The Nd^{III} ions and L^{3-} ligands are marked in pink and blue, respectively.

Complexes **1** (Pr), **3** (Sm), and **4** (Eu) have similar structures to that of **2** (Nd), except that the bond lengths and bond angles are slightly different from those of **2.** All of these values decrease from **1** to **4**, which is agreement with the radius contraction of the lanthanide metal centers.

Crystal structures of 5 and 6 (type II)

The X-ray crystallographic analyses revealed that complexes **5** and **6** were also isostructural and possessed a 3D framework structure that differed from that of **1**–**4** and belongs to the monoclinic system in the *C*2/*c* space group. Therefore, the structure of compound **5** is described as an example. There are two and half Tb^{III} ions, two L^{3-} anions, one and half formate anions, two coordination water molecules, and five lattice water molecules in the asymmetric unit. As shown in Figure 2a, Tb1 is nonacoordinated with O1, O3, O13, O15, O17, and O18, which belong to one L^{3-} ligand, two formate anions, two coordination water molecules, and three nitrogen atoms (N1, N2, and N3), which belong to one L^{3-} to form a distorted tetrakaidecahedron coordination geometry. Tb2 is octacoordinated with four oxygen atoms (O7, O9, O12, and O14), which belong to two L^{3-} ligands and one formate anion, and four nitrogen atoms (N5, N6, N7, and N8), which belong to two L^{3-} li-

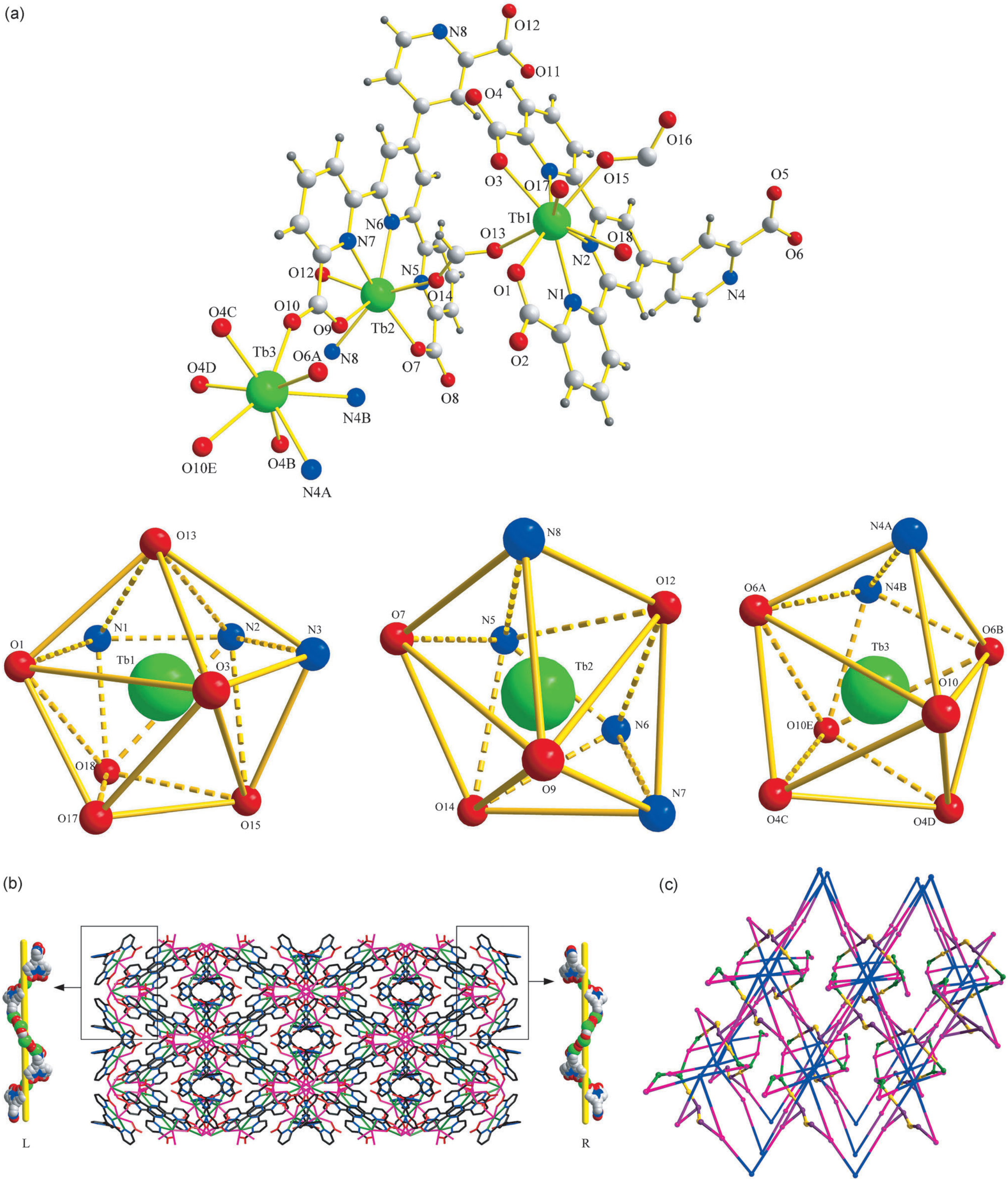

Figure 2. a) Representation of the Tb^{III} coordination environments in **5**. b) View of the helical chains and the 3D network in **5**. c) View of the 3D topological network in **5**. Tb1, Tb2, Tb3, COO^- anions, and L^{3-} anions are marked in violet, green, blue, gold, and pink, respectively.

gands. Tb3 is octacoordinated with six oxygen atoms (O10, O6A, O6B, O4C, O4D, and O10E), which belong to six L^{3-} ligands, and two nitrogen atoms (N4A and N4B), which belong to two L^{3-} ligands. The coordination geometry of Tb2 and Tb3 is a distorted square antiprism. The Tb–O bond lengths are in the range of 2.269(9) to 2.559(8) Å, and the Tb–N bond lengths are in the range of 2.496(4) and 2.595(4) Å. The pyridyl rings of two crystallographically independent L^{3-} anions are nonplanar. The N4 pyridyl ring is twisted with respect to the central pyridyl ring (N2 pyridyl) with a dihedral angle of 54.11° and the N8

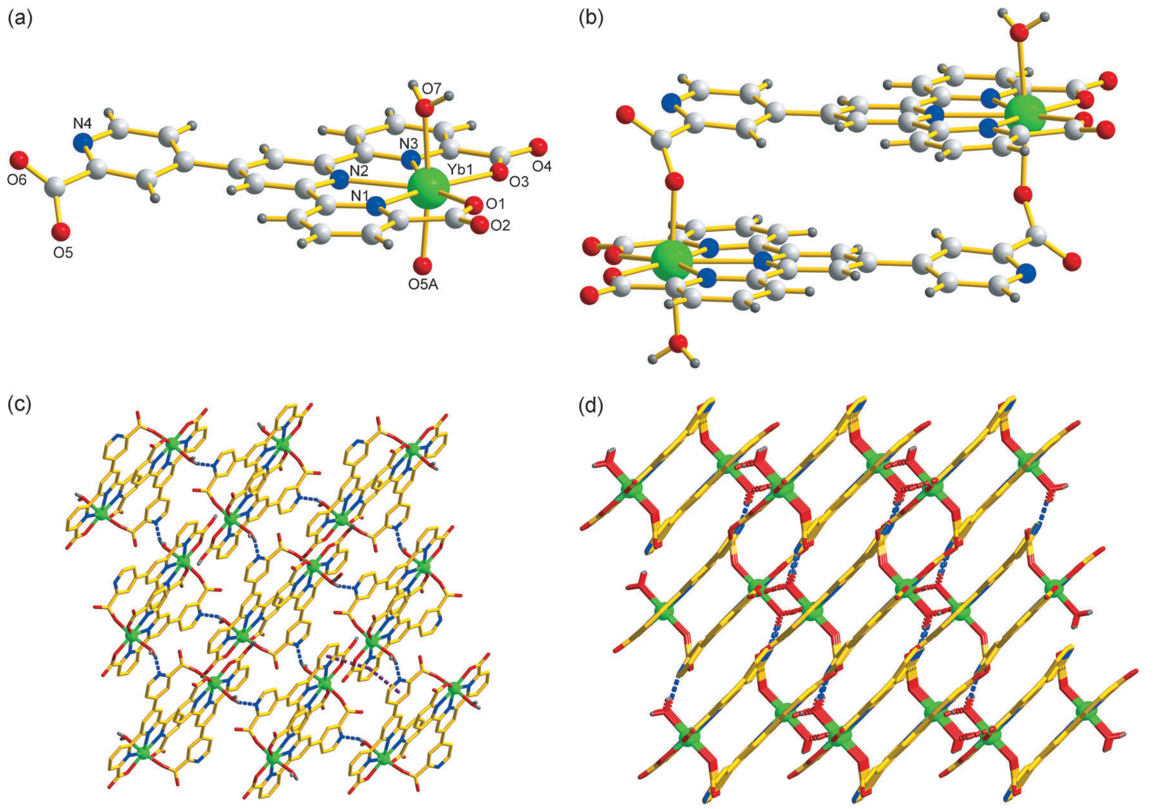

Figure 3. a) The coordination environment of Yb^{III} in **7**. b) View of the dinuclear structure of **7**. c) View of the 2D supramolecular structure in **7**. d) View of the 3D supramolecular network in **7**. The O7–H7B···N4 hydrogen bonds are colored blue and the O7–H7A···O4 hydrogen bonds are colored red.

pyridyl ring is twisted with respect to the central pyridyl ring (N6 pyridyl) with a dihedral angle of 46.05°.

In compound **5**, the Tb^{III} centers are interconnected by bridging carboxylate groups of the L^{3-} anions and the COO^- anion to form infinite one-dimensional helical chains running along the *c* axis (Figure 2b). It is interesting that there are right-handed helical chains and left-handed helical chains appearing alternately in compound **5**. An individual strand has a repeat unit consisting of Tb3-O-C-O-Tb2-COO^--Tb1-COO^--Tb1-COO^--Tb2-O-C-O-Tb3. Tb1 ions are linked to Tb1 and Tb2 ions by COO^- anions. Tb2 and Tb3 ions are linked by the carboxylate groups of L^{3-} anions. The nearest Tb3–Tb2, Tb2–Tb1, and Tb1–Tb1 distances are 16.346(9), 6.754(4), and 6.162 (7) Å. The adjacent helical chains are further assembled through L^{3-} anions into a three-dimensional framework. To better understand the complicated framework, the network topology in complex **5** was analyzed. If Tb1, Tb2, and Tb3 are considered as three-, three-, and six-connected nodes, whereas the core of the COO^- anion core and the core of the ligand core are considered as two- and three-connected nodes, respectively, the complicated architecture of **5** is simplified into a new 3D topological network with the Schläfli symbol of $(5.7.8)_2(5.7^2.8^6.10^2.11^4)(5.8.9)_2(7^2.10)_2(7^2.8)_2$, as shown in Figure 2c.

Crystal structure of 7 (type III)

Complex **7** crystallizes in the monoclinic $P2_1/c$ space group and is dinuclear in structure. In the asymmetric unit, there is one Yb^{III} ion, one L^{3-} anion, one coordination water molecule, and one lattice water molecule. As shown in Figure 3a, the Yb^{III} center is coordinated to three oxygen atoms (O1, O3, and O5A), which belong to two symmetry-related L^{3-} ligands; three nitrogen atoms (N1, N2, and N3), which belong to one L^{3-} ligand, and one coordination water molecule (O1W). This coordination leads to a distorted pentagonal bipyramidal geometry. The Yb–O bond lengths are in the range of 2.151(2) to 2.267(2) Å, and the Yb–N distances fall in the range of 2.384(3)–2.440(3) Å, which are similar to those observed in other Yb^{III} coordination polymers.[16] Two Yb^{III} ions are bridged by a pair of L^{3-} ligands to form a discrete dinuclear structure (Figure 3b). The Yb–Yb distance is 10.511(2) Å. The 2D supramolecular sheet is constructed through hydrogen-bonding interactions between the coordinated water molecules and the pyridyl nitrogen atoms of the L^{3-} ligands ($O7–H7B···N4^i$, 2.718 Å, 161.8°, symmetry code: $i = -x+1, y-1/2, -z+3/2$), as shown in Figure 3c. The sheets are also supported by π–π interactions. There are two weak intermolecular π–π stacking interactions (Figure S2 in the Supporting Information). One type of π–π stacking interaction exists between the outer N3 pyridyl and terminal N4 pyridyl rings, with a centroid to centroid distance of 3.586 Å. Another centroid–centroid distance is 3.471 Å. Finally, a 3D supramolecular structure is formed through O7—H7A···O4^{ii} (2.763 Å, 170.5°, symmetry code: ii: $-x+2$, $-y$, $-z+2$) hydrogen bonds (Figure 3 d).

In complexes **1**–**7**, the average Ln—O bond lengths (from **1** (Pr; 2.464 Å) to **7** (Yb; 2.224 Å)) and the average Ln—N bond lengths (from **1** (Pr; 2.718 Å) to **7** (Yb; 2.403 Å)) decrease as the atomic number increases, which demonstrates the existence of a lanthanide contraction effect. Simultaneously, the coordination number decreases from nine to seven as the atomic number of the lanthanide metal ions increases from Pr^{III} to Yb^{III}. The change in the coordination number of the lanthanide metal ions leads to different geometries for the lanthanide ions and the crystal structures of the lanthanide complexes. This difference may be due to the larger ionic radius and lower electronic density of Nd^{III} relative to Yb^{III}, which allows a higher coordination number for the former. This result implies that complexes of lanthanide ions with the same ligand throughout the series from the same reaction process may have different atomic coordination owing to the lanthanide contraction effect that results from different lanthanide ions.

IR spectroscopy

The structures of compounds **1**–**7** were confirmed by IR spectroscopy. All of the spectra exhibit a broad band ($\tilde{\nu}=2800$–$3700\ cm^{-1}$) that corresponds to ν_{O-H} stretching vibrations of water molecules. The absence of any strong bands near $\tilde{\nu}=1700\ cm^{-1}$ for **1**–**7** indicates that the carboxyl group of the ligand is completely deprotonated.[17] The bands at $\tilde{\nu}=1580$–1635 and 1360–1490 cm^{-1} are due to the asymmetric stretching and symmetric stretching of carboxylate groups, respectively. The difference between ν_{as} and ν_s of 246 (**1**–**6**) and 210 cm^{-1} (**7**) is more than 200 cm^{-1}, which indicates monochelation of the carboxyl group to the metal ion, in agreement with X-ray diffraction analysis. The bands in the region of $\tilde{\nu}=650$–$1300\ cm^{-1}$ for **1**–**7** were assigned to the CH in- or out-of-plane bending, ring breathing, and ring deformation absorptions of the pyridyl ring.

Thermal stabilities

The isostructural frameworks lead to similar thermal decomposition processes, so we took complexes **1**, **5**, and **7** as representative examples for thermogravimetric analysis (TGA). As shown in Figure S3 in the Supporting Information, complex **1** lost its uncoordinated water molecules below 200 °C. The weight loss of 3.20 % is consistent with the calculated value (3.06 %). The framework is stable up to 530 °C and then the framework begins to collapse. For complex **5**, continuous weight losses below approximately 290 °C correspond to the loss of all of the lattice water and coordinated water molecules (calcd: 8.65 %; found: 8.84 %). The COO^- anions and L^{3-} ligands start to leave the framework above 420 °C. The thermal stability of **7** indicates that the uncoordinated water and coordinated waters molecules are removed below 260 °C (calcd: 4.94 %; found: 5.09 %). At 490 °C, these complexes gradually decompose.

Luminescent properties

The lanthanide coordination polymers have shown good luminescence properties. Hence, the photoluminescence properties of the lanthanide complexes and the free ligand are investigated in the solid state at room temperature, as depicted in Figure 4 and Figure S4 in the Supporting Information. Complexes **3**–**6** exhibit characteristic emissions of Ln^{III} ions in the visible region. Complexes **2** and **7** show characteristic emissions of Nd^{III} and Yb^{III} ions in the NIR region. The free ligand exhibits one strong emission band at $\lambda=460$ nm upon excitation at $\lambda=310$ nm. For complex **1**, no emission band in the NIR region was found. Compound **2** shows three typical NIR emission bands of Nd^{III} ($\lambda=918$, 1060, and 1329 nm), which are assigned to the $^4F_{3/2}\rightarrow{}^4I_{J/2}$ ($J=9$, 11, 13) transitions upon excitation at $\lambda=298$ nm.[18] For the emission spectrum of complex **7**, the Yb^{III} ion emits a sharp peak at $\lambda=980$ nm excited with $\lambda=298$ nm light, which is assigned to the $^2F_{5/2}\rightarrow{}^2F_{7/2}$ transition of the broader vibronic components of the Yb^{III} ions at a longer wavelength.[19] The Yb^{III} ion plays an important role in laser emission because of its very simple f–f energy level structure.

Complex **3** exhibits an orange emission with three characteristic Sm^{III} bands at $\lambda=561$, 595, and 642 nm, which are attributed to radiative decay from the $^4G_{5/2}$ level to the $^6H_{5/2}$, $^6H_{7/2}$, and $^6H_{9/2}$ levels, respectively, as observed for other Sm^{III} compounds.[20] The corresponding luminescence decay profiles of complexes **3**–**6** are shown in Figure S5 in the Supporting Information. All data were well fitted by a double exponential function. For complex **3**, the emission intensity is fractioned into two amplitudes with different magnitudes. They are represented by pre-exponential values A_1 and A_2, which correspond to the decay times τ_1 and τ_2, respectively. The average lifetime τ_{av} is given by $\tau_{av}=(A_1\tau_1{}^2+A_2\tau_2{}^2)/(A_1\tau_1+A_2\tau_2)$. The Sm^{III} lifetime is measured to be $\tau_1=4.72\ \mu s$, $A_1=0.9282$; $\tau_2=13.79\ \mu s$, $A_2=0.0718$; $\tau_{av}=6.39\ \mu s$.

If **4** is excited at $\lambda=256$ nm, the excitation peaks at $\lambda=591$, 617, 650, and 699 nm can be attributed to $^5D_0\rightarrow{}^7F_1$, $^5D_0\rightarrow{}^7F_2$, $^5D_0\rightarrow{}^7F_3$, and $^5D_0\rightarrow{}^7F_4$ transitions, respectively, of complex **4**. This $^5D_0\rightarrow{}^7F_2$ transition dominates the red emission light. The intensity of the $^5D_0\rightarrow{}^7F_2$ transition (induced electric dipole transition) is much more intense than the $^5D_0\rightarrow{}^7F_1$ transition (magnetic dipole transition), which indicates that the coordination environment of the Eu^{III} ion is asymmetric.[21] The lifetimes for **4** are $\tau_1=184.53\ \mu s$, $A_1=0.4356$; $\tau_2=489.86\ \mu s$, $A_2=0.5644$; $\tau_{av}=421.31\ \mu s$.

Upon excitation at $\lambda=256$ nm, four characteristic peaks of complex **5** at $\lambda=491$, 545, 584, and 621 nm are assigned to the $^5D_4\rightarrow{}^7F_6$, $^5D_4\rightarrow{}^7F_5$, $^5D_4\rightarrow{}^7F_4$, and $^5D_4\rightarrow{}^7F_3$ transitions, respectively.[22] The Tb^{III} lifetime is measured to be $\tau_1=24.49\ \mu s$, $A_1=0.5268$; $\tau_2=55.91\ \mu s$, $A_2=0.4732$; $\tau_{av}=45.61\ \mu s$. For **6**, the characteristic luminescent bands of the dysprosium complex were recorded at $\lambda=485$ and 562 nm through the ligand-to-metal energy-transfer mechanism, which could be attributed to $^4G_{5/2}\rightarrow{}^6H_{7/2}$ and $^4G_{5/2}\rightarrow{}^6H_{7/2}$.[23] The Dy^{III} lifetime is measured to be $\tau_1=3.1\ \mu s$, $A_1=0.7946$; $\tau_2=9.47\ \mu s$, $A_2=0.2054$; $\tau_{av}=5.91\ \mu s$.

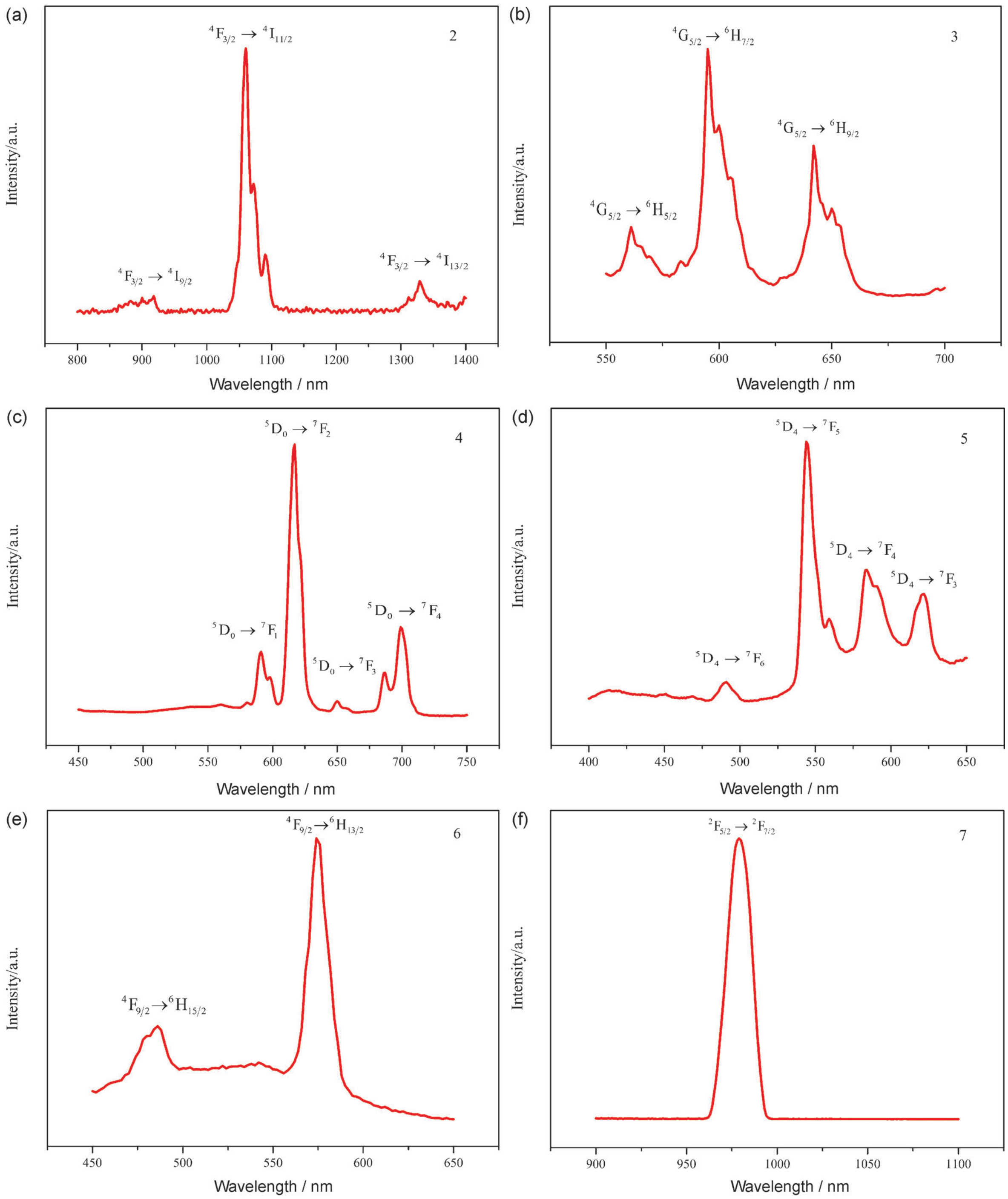

Figure 4. The emission spectra of a) **2**, b) **3**, c) **4**, d) **5**, e) **6**, and f) **7** in the solid state at room temperature.

Conclusion

We reported the syntheses and crystallographic analysis of seven new lanthanide–ligand complexes. These complexes, which were synthesized with the H_3L ligand and different lanthanide chlorides by a solvothermal reaction, crystallized into three structural types as follows: type I for the large ions, Pr^{III}, Nd^{III}, Sm^{III} and Eu^{III}; type II for the medium ions, Tb^{III} and Dy^{III}; and type III for the small ion, Yb^{III}. All complexes exhibited very high thermal stability and the photoluminescence properties were also discussed. Complexes **2**–**7** exhibited characteristic luminescent properties of neodymium, samarium, europium, terbium, dysprosium, and ytterbium, which indicated that Ln^{III} ions were efficiently sensitized by the ligand. Our studies also showed that complexes **3**–**6** had lifetimes on the microsecond level, and thus, might become promising candidates for luminescent materials.

Experimental Section

Materials and methods

The H_3L ligand was prepared according to the literature with some modifications (Scheme 1).[24–27] All other chemicals were obtained from commercial sources without further purification. Elemental analyses (C, H, and N) were recorded on an Elementar Vario EL III elemental analyzer. ^1H and ^{13}C NMR spectra were recorded at room temperature by using a Varian Inova 400 MHz apparatus and tetramethylsilane (TMS) as a reference. The IR spectra were recorded as KBr pellets on a Bruker EQUINOX 55 Fourier transform infrared spectrometer in the range of 400–4000 cm^{-1}. The emission spectra were recorded on a Hitachi F-4500 spectrophotometer in the solid state at room temperature. TGA was performed with a Universal V2.6 DTA instrument under an N_2 atmosphere at a heating rate of 10 °C min^{-1}.

Synthesis

4′-(4-*N*-oxypyridyl)-2,2′:6′,2″-terpyridine-1,1″-di-*N*-oxide: 4′-Pyridyl-2,2′:6′,2″-terpyridine (0.93 g, 3 mmol) and mCPBA (0.774 g, 4.5 mmol) in CH_2Cl_2 (80 mL) were stirred at room temperature for 24 h. Yellow precipitate was filtered off, recrystallized with ethanol and DMF, and dried in vacuo to yield a yellow powder (0.79 g, 74 %). M.p. 245–246 °C; ^1H NMR (400 MHz, [D$_6$]DMSO): $\delta = 9.10$ (s, 1 H), 8.44 (d, $J = 12.0$ Hz, 1 H), 8.38 (d, $J = 8.0$ Hz, 1 H), 8.22 (d, $J =$ 4.0 Hz, 8.0 Hz, 1 H), 7.91 (d, $J = 8.0$ Hz, 2 H), 7.54 ppm (t, $J = 4.0$, 8.0 Hz, 2 H); ^{13}C NMR (400 MHz, [D$_6$]DMSO): $\delta = 169.8$, 150.1, 145.2, 140.0, 139.1, 132.4, 127.5, 126.3, 125.2, 124.0, 121.7 ppm; IR (KBr): $\tilde{\nu} = 3419$, 3109, 3075, 2027, 1617, 1540, 1485, 1444, 1397, 1259, 1190, 1112, 1083, 1030, 842, 802, 766, 715, 637, 582, 475 cm^{-1}; elemental analysis calcd (%) for $C_{20}H_{14}N_4O_3$ (358.36): C 67.03, H 3.94, N 15.63; found: C 67.26, H 3.92, N 15.45.

4′-(3-pyridylacetonitrile)-2,2′:6′,2″-terpyridine-6,6″-dicarbonitrile: 4′-(3-*N*-Oxypyridyl)-2,2′:6′,2″-terpyridine-1,1″-di-*N*-oxide (0.72 g, 2 mmol) and Me_3SiCN (0.891 g, 9 mmol) were added to CH_2Cl_2 (100 mL). After stirring for 30 min, benzoyl chloride was added over the course of 30 min. After stirring for 48 h at room temperature, the mixture was evaporated to half its volume. K_2CO_3 (100 mL, 0.8 mol L^{-1}) was added, and the mixture was stirred for 1 h. The precipitate was filtered and washed with H_2O and cold CH_2Cl_2. The white precipitate was recrystallized with ethanol and DMF, and dried in vacuo to yield a white powder (0.53 g, 68 %). M.p. 263–265 °C; ^1H NMR (400 MHz, [D$_6$]DMSO): $\delta = 9.02$ (d, $J =$ 8.0 Hz, 1 H), 8.95 (s, 1 H), 8.84 (s, 1 H), 8.80 (s, 1 H), 8.39 (s 1 H), 8.33 (d, $J = 8.0$ Hz, 1 H), 8.24 ppm (d, $J = 8.0$ Hz, 1 H); IR (KBr): $\tilde{\nu} = 3447$, 3072, 2851, 2237, 2025, 1639, 1577, 1539, 1455, 1389, 1274, 1126 1080, 988, 904, 858, 819, 739, 635, 575, 468 cm^{-1}; elemental analysis calcd (%) for $C_{23}H_{11}N_7$ (385.39): C 71.68, H 2.88, N 25.44; found: C 71.83, H 2.85, N 25.32.

4′-(3-carboxylpyridyl)-2,2′:6′,2″-terpyridine-6,6″-dicarboxylic acid: KOH was added as a base to a solution of 4′-(3-pyridylacetonitrile)-2,2′:6′,2″-terpyridine-6,6″-dicarbonitrile (0.39 g, 1 mmol) in ethanol/H_2O (v/v, 4:1, 50 mL). The reaction mixture was heated at reflux for 6 h. Then, the pH was adjusted to three with an aqueous solution of HCl (1 mol L^{-1}). The yellow precipitate was filtered, recrystallized with ethanol and DMF, and dried in vacuo to yield a yellow powder (0.36 g, 81 %). M.p. 265–267 °C; ^1H NMR (400 MHz, [D$_6$]DMSO): $\delta = 12.85$ (s, 1 H), 9.12 (s, 2 H), 8.88 (m, 4 H), 8.58 (m, 1 H), 8.21 (d, $J = 32$ Hz, 3 H), 7.88 ppm (d, $J = 44$ Hz, 1 H); ^{13}C NMR (400 MHz, [D$_6$]DMSO): $\delta = 171.3$, 171.1, 170.9, 160.3, 160.1, 159.6, 158.9, 155.8, 155.6, 155.4, 154.7, 152.9, 152.0, 151.2, 144.3, 144.1, 130.5, 130.1, 129.5, 128.7, 127.9, 127.5, 124.5 ppm; IR (KBr): $\tilde{\nu} =$ 3442, 3325, 2774, 2464, 1712, 1644, 1583, 1541, 1451, 1380, 1222, 1144, 1077, 994, 897, 835, 783, 741, 682, 635, 487 cm^{-1}; elemental analysis calcd (%) for $C_{23}H_{14}N_4O_6$ (442.39): C 62.45, H 3.19, N 12.66; found: C 62.69, H 3.22, N 12.45.

Synthesis of 1–4 and 7: In a typical reaction, a mixture of $NdCl_3 \cdot 6H_2O$ (0.25 mmol) and H_3L (0.25 mmol) was placed in a Teflon-lined stainless-steel vessel (25 mL) with DMF/H_2O (3:7, v/v, 10 mL). The mixture was heated to 160 °C over the course of 6 h and maintained at this temperature for 3 days. After cooling to room temperature at a rate of 5 °C h^{-1}, yellow block crystals of **2** were obtained (yield 49 % based on $NdCl_3 \cdot 6H_2O$). IR (KBr) for **2**: $\tilde{\nu} =$ 3419, 1618, 1585, 1424, 1371, 1268, 1228, 1173, 1082, 1007, 923, 854, 790, 733, 706, 657, 628, 551 cm^{-1}; elemental analysis calcd (%) for $C_{46}H_{22}N_8O_{13}Nd_2$ (1183.21): C 46.70, H 1.87, N 9.47; found: C 46.95, H 1.89, N 9.36.

Yellow block crystals of **1**, **3**, **4**, and **7** were obtained in moderate yields (36 %–63 %) by a similar method to that described for **2**, except that the corresponding $LnCl_3 \cdot 6H_2O$ was used instead of $NdCl_3 \cdot 6H_2O$. For **1**: IR (KBr): $\tilde{\nu} = 3419$, 1618, 1585, 1424, 1371, 1268, 1228, 1173, 1082, 1007, 923, 854, 790, 733, 706, 657, 628, 551 cm^{-1}; elemental analysis calcd (%) for $C_{46}H_{22}N_8O_{13}Pr_2$ (1176.54): C 46.96, H 1.88, N 9.52; found: C 47.14, H 1.91, N 9.67. For **3**: IR (KBr): $\tilde{\nu} =$ 3419, 1618, 1585, 1424, 1371, 1268, 1228, 1173, 1082, 1007, 923, 854, 790, 733, 706, 657, 628, 551 cm^{-1}; elemental analysis calcd (%) for $C_{46}H_{22}N_8O_{13}Sm_2$ (1195.45): C 46.22, H 1.85, N 9.37; found: C 45.94, H 1.82, N 9.22. For **4**: IR (KBr): $\tilde{\nu} = 3419$, 1618, 1585, 1424, 1371, 1268, 1228, 1173, 1082, 1007, 923, 854, 790, 733, 706, 657, 628, 551 cm^{-1}; elemental analysis calcd (%) for $C_{46}H_{22}N_8O_{13}Eu_2$ (1198.66): C 45.49, H 1.83, N 9.23; found: C 45.17, H 1.85, N 9.08. For **7**: IR (KBr): $\tilde{\nu} = 3512$, 3413, 3074,1659, 1594, 1537, 1482, 1449, 1414, 1345, 1270, 1181, 1081, 1022, 924, 865, 796, 734, 702, 661, 635, 576, 462, 425 cm^{-1}; elemental analysis calcd (%) for $C_{46}H_{30}N_8O_{16}Yb_2$ (1296.87): C 42.60, H 2.33, N 8.64; found: C 42.92, H 2.35, N 8.76.

Synthesis of 5 and 6: The procedure is similar to that described for **2**. If $NdCl_3 \cdot 6H_2O$ in **2** was replaced with $TbCl_3 \cdot 6H_2O$ and $DyCl_3 \cdot 6H_2O$ and the reaction temperature was adjusted to 180 °C, two completely different compounds, **5** and **6**, were obtained. For **5**: IR (KBr): $\tilde{\nu} = 3450$, 2026, 1620, 1589, 1428, 1374, 1272, 1173, 1010, 851, 792, 708, 628 cm^{-1}; elemental analysis calcd (%) for $C_{95}H_{46}N_{16}O_{44}Tb_5$ (2910.08): C 39.21, H 1.59, N 7.70; found: C 39.34, H 1.57, N 7.82. For **6**: IR (KBr): $\tilde{\nu} = 3450$, 2026, 1620, 1589, 1428, 1374, 1272, 1173, 1010, 851, 792, 708, 628 cm^{-1}; elemental analysis calcd (%) for $C_{95}H_{46}N_{16}O_{44}Dy_5$ (2927.99): C 38.97, H 1.58, N 7.65; found: C 38.92, H 1.57, N 7.69.

X-ray crystallography

Single-crystal X-ray diffraction measurements for **1**–**7** were performed on a Bruker Smart Apex II CCD diffractometer using graphite monochromatic Mo Kα radiation ($\lambda = 0.71073$ Å) at 296 K. The structures were solved by direct methods and refined by full-matrix least-squares on F^2 with the SHELX-97 program.[28] The metal atoms were located from the E-maps, and the other non-hydrogen atoms were located in successive difference Fourier syntheses. All non-hydrogen atoms were refined with anisotropic thermal parameters. The hydrogen atoms on the carbon atoms were positioned geometrically. The crystallographic data and structural refinements for **1**–**7** are listed in Table 1. Selected bond lengths and angles for **1**–**7** are listed in Table S1 in the Supporting Information.

Table 1. Crystallographic data and structural refinement parameters for **1**–**7**.

Complex	1	2	3	4	5	6	7
empirical formula	$C_{46}H_{22}N_8O_{13}Pr_2$	$C_{46}H_{22}N_8O_{13}Nd_2$	$C_{46}H_{22}N_8O_{13}Sm_2$	$C_{46}H_{22}N_8O_{13}Eu_2$	$C_{95}H_{46}N_{16}O_{44}Tb_5$	$C_{95}H_{46}N_{16}O_{44}Dy_5$	$C_{46}H_{30}N_8O_{16}Yb_2$
formula weight	1176.54	1183.20	1195.42	1214.64	2910.13	2927.98	1296.86
T [K]	296(2)	296(2)	296(2)	296(2)	296(2)	296(2)	296(2)
crystal system	monoclinic	monoclinic	monoclinic	monoclinic	monoclinic	monoclinic	monoclinic
space group	$P2_1/c$	$P2_1/c$	$P2_1/c$	$P2_1/c$	$C2/c$	$C2/c$	$P2_1/c$
a [Å]	11.3714(12)	11.3195(11)	11.3314(8)	11.3224(8)	15.5659(12)	15.5149(11)	9.7382(9)
b [Å]	19.825(2)	19.685(2)	19.6533(13)	19.6273(13)	29.759(2)	29.726(2)	13.5199(12)
c [Å]	9.5422(10)	9.4765(10)	9.4923(6)	9.4741(6)	22.7134(19)	22.6206(17)	16.6137(15)
α [°]	90	90	90	90	90	90	90
β [°]	106.822(1)	106.885(1)	107.174(1)	107.212(1)	97.155(1)	97.549(1)	103.006(1)
γ [°]	90	90	90	90	90	90	90
V [Å^3]	2059.1(4)	2020.5(4)	2019.67(20)	2011.1(2)	10439.4(14)	10342.0(13)	2131.2(3)
Z	2	2	2	2	4	4	2
ρ_{calcd} [g cm^{-3}]	1.898	1.945	1.966	2.006	1.852	1.881	2.021
μ [mm^{-1}]	2.421	2.625	2.963	3.178	3.443	3.669	4.450
F (000)	1152	1156	1164	1184	5620	5640	1260
GOF	1.073	1.091	1.000	1.017	1.041	1.056	1.000
reflns collected	10180	10004	10010	10017	26025	27272	10437
reflns unique	3637	3558	3567	3553	9198	9829	3751
R_{int}	0.0278	0.0214	0.0196	0.0386	0.0280	0.0480	0.0217
R_1[a], wR_2[b] [$I>2\sigma(I)$]	0.0267, 0.0675	0.0238, 0.0582	0.0260, 0.0886	0.0283, 0.0574	0.0322, 0.0810	0.0468, 0.1367	0.0218, 0.0552
R_1[a], wR_2[b] (all data)	0.0281, 0.0684	0.0256, 0.0591	0.0275, 0.0902	0.0397, 0.0617	0.0391, 0.0853	0.0648, 0.1615	0.0240, 0.0562

[a] $R=\Sigma \| F_0 \| - \| F_C \| / \Sigma \| F_0 \|$. [b] $wR_2 = \{\Sigma[w(F_0^2 - F_C^2)^2]/\Sigma[(F_0^2)^2]\}^{1/2}$.

Acknowledgements

This study was supported by the National Natural Science Foundation of China (grant nos. 20873098 and 21173164).

Keywords: lanthanides · ligand design · luminescence · metal–organic frameworks · polymers

[1] a) D. Maspoch, D. Ruiz-Molina, J. Veciana, *Chem. Soc. Rev.* **2007**, *36*, 770–818; b) M. D. Allendorf, C. A. Bauer, R. K. Bhakta, R. J. T. Houk, *Chem. Soc. Rev.* **2009**, *38*, 1330–1352; c) R. J. Kuppler, D. J. Timmons, Q. R. Fang, J. R. Li, T. A. Makal, M. D. Young, D. Q. Yuan, D. Zhao, W. J. Zhuang, H. C. Zhou, *Coord. Chem. Rev.* **2009**, *253*, 3042–3066; d) L. E. Kreno, K. Leong, O. K. Farha, M. Allendorf, R. P. Van Duyne, J. T. Hupp, *Chem. Rev.* **2012**, *112*, 1105–1125.

[2] a) C. Wang, T. Zhang, W. B. Lin, *Chem. Rev.* **2012**, *112*, 1084–1104; b) Y. Cui, Y. Yue, G. Qian, B. Chen, *Chem. Rev.* **2012**, *112*, 1126–1162; c) S. T. Meek, J. A. Greathouse, M. D. Allendorf, *Adv. Mater.* **2011**, *23*, 249–267; d) P. Wu, J. Wang, Y. Li, C. He, Z. Xie, C. Duan, *Adv. Funct. Mater.* **2011**, *21*, 2788–2794; e) B. Chen, L. Wang, F. Zapata, G. Qian, E. B. Lobkovsky, *J. Am. Chem. Soc.* **2008**, *130*, 6718–6719.

[3] a) Z. H. Zhang, Y. Song, T. Okamura, Y. Hasegawa, W. Y. Sun, N. Ueyama, *Inorg. Chem.* **2006**, *45*, 2896–2902; b) K.-L. Wong, G.-L. Law, Y.-Y. Yang, W.-T. Wong, *Adv. Mater.* **2006**, *18*, 1051–1054; c) Z. Y. Li, G. S. Zhu, X. D. Guo, X. J. Zhao, Z. Jin, S. L. Qiu, *Inorg. Chem.* **2007**, *46*, 5174–5178; d) B. V. Harbuzaru, A. Corma, F. Rey, P. Atienzar, J. L. Jordá, H. García, D. Ananias, L. D. Carlos, J. Rocha, *Angew. Chem.* **2008**, *120*, 1096–1099; *Angew. Chem. Int. Ed.* **2008**, *47*, 1080–1083; e) B. Chen, L. Wang, Y. Xiao, F. R. Fronczek, M. Xue, Y. Cui, G. Qian, *Angew. Chem.* **2009**, *121*, 508–511; *Angew. Chem. Int. Ed.* **2009**, *48*, 500–503; f) X. Zhang, M. A. Ballem, Z.-J. Hu, P. Bergman, K. Uvdal, *Angew. Chem.* **2011**, *123*, 5847–5851; *Angew. Chem. Int. Ed.* **2011**, *50*, 5729–5733.

[4] Y.-F. Liu, G. F. Hou, Y. H. Yu, P. F. Yan, J. Y. Li, G. M. Li, J. S. Gao, *Cryst. Growth Des.* **2013**, *13*, 3816–3824.

[5] a) X. H. Bu, W. Chen, W. F. Hou, M. Du, R. H. Zhang, F. Brisse, *Inorg. Chem.* **2002**, *41*, 3477–3482; b) H. L. Jiang, Y. Tatsu, Z. H. Lu, Q. Xu, *J. Am. Chem. Soc.* **2010**, *132*, 5586–5587; c) W. G. Lu, L. Jiang, X.-L. Feng, T.-B. Lu, *Inorg. Chem.* **2009**, *48*, 6997–6999; d) J. Rocha, L. D. Carlos, F. A. Paz, D. Ananias, *Chem. Soc. Rev.* **2011**, *40*, 926–940; e) X.-Q. Song, X.-Y. Zhou, W.-S. Liu, W. Dou, J.-X. Ma, X.-L. Tang, J.-R. Zheng, *Inorg. Chem.* **2008**, *47*, 11501–11513.

[6] a) K. Bernot, L. Bogani, A. Caneschi, D. Gatteschi, R. Sessoli, *J. Am. Chem. Soc.* **2006**, *128*, 7947–7956; b) Y. Q. Sun, J. Zhang, Y. M. Chen, G. Y. Yang, *Angew. Chem.* **2005**, *117*, 5964–5967; *Angew. Chem. Int. Ed.* **2005**, *44*, 5814–5817; c) A. Kobayashi, Y. Suzuki, T. Ohba, S. I. Noro, H. C. Chang, M. Kato, *Inorg. Chem.* **2011**, *50*, 2061–2063; d) Q. H. Xu, L. S. Li, X. S. Liu, R. R. Xu, *Chem. Mater.* **2002**, *14*, 549–555; e) N. Kerbellec, D. Kustaryono, V. Haquin, M. Etienne, C. Daiguebonne, O. Guillou, *Inorg. Chem.* **2009**, *48*, 2837–2843.

[7] a) K. Binnemans, *Chem. Rev.* **2009**, *109*, 4283–4374; b) G. M. Farinola, R. Ragni, *Chem. Soc. Rev.* **2011**, *40*, 3467–3482; c) J. Kido, Y. Okamoto, *Chem. Rev.* **2002**, *102*, 2357–2368; d) K. Kuriki, Y. Koike, Y. Okamoto, *Chem. Rev.* **2002**, *102*, 2347–2356; e) S. V. Eliseeva, J. C. G. Bunzli, *Chem. Soc. Rev.* **2010**, *39*, 189–227; f) H. Kobayashi, M. Ogawa, R. Alford, P. L. Choyke, Y. Urano, *Chem. Rev.* **2010**, *110*, 2620–2640; g) R. W. Sinkeldam, N. J. Greco, Y. Tor, *Chem. Rev.* **2010**, *110*, 2579–2619.

[8] a) M. P. Lowe, D. Parker, O. Reany, S. Aime, M. Botta, G. Castellano, E. Gianolio, R. Pagliarin, *J. Am. Chem. Soc.* **2001**, *123*, 7601–7609; b) S. Blair, M. P. Lowe, C. E. Mathieu, D. Parker, P. K. Senanayake, R. Kataky, *Inorg. Chem.* **2001**, *40*, 5860–5867; c) M. Elbanowski, B. J. Makowska, *J. Photochem. Photobiol. A* **1996**, *99*, 85–92.

[9] a) W. Huang, D. Y. Wu, P. Zhou, W. B. Yan, D. Guo, C. Y. Duan, Q. Meng, *Cryst. Growth Des.* **2009**, *9*, 1361–1369; b) W. S. Liu, T. Q. Jiao, Y. Z. Li, Q. Z. Liu, M. Y. Tan, H. Wang, L. F. Wang, *J. Am. Chem. Soc.* **2004**, *126*, 2280–2281.

[10] a) H. C. Aspinall, *Chem. Rev.* **2002**, *102*, 1807–1850; b) A. de Bettencourt-Dias, A. Poloukhtine, *J. Phys. Chem. B* **2006**, *110*, 25638–25645; c) S. Viswanathan, A. de Bettencourt-Dias, *Inorg. Chem.* **2006**, *45*, 10138–10146; d) D. Parker, R. S. Dickins, H. Puschmann, C. Crossland, J. A. K. Howard, *Chem. Rev.* **2002**, *102*, 1977–2010; e) C. Marchal, Y. Filinchuk, X. Y. Chen, D. Imbert, M. Mazzanti, *Chem. Eur. J.* **2009**, *15*, 5273–5288.

[11] a) J. Zhang, P. D. Badger, S. J. Geib, S. Petoud, *Angew. Chem.* **2005**, *117*, 2564–2568; *Angew. Chem. Int. Ed.* **2005**, *44*, 2508–2512; b) J.-C. G. Bünzli, C. Piguet, *Chem. Rev.* **2002**, *102*, 1897; c) H. Tsukube, S. Shinoda, *Chem. Rev.* **2002**, *102*, 2389–2403.

[12] a) M. Hilder, P. C. Junk, U. H. Kynast, M. M. Lezhnina, *J. Photochem. Photobiol. A* **2009**, *202*, 10 – 20; b) V. Tsaryuk, K. Zhuravlev, V. Zolin, P. Gawryszewska, J. Legendziewicz, V. Kudryashova, I. Pekareva, *J. Photochem. Photobiol. A* **2006**, *177*, 314 – 323.

[13] A. de Bettencourt-Dias, S. Viswanathan, *Dalton Trans.* **2006**, 4093 – 4103.

[14] a) J. Ye, J. Zhang, G. Ning, G. Tian, Y. Chen, Y. Wang, *Cryst. Growth Des.* **2008**, *8*, 3098 – 3106; b) M. S. Liu, Q. Y. Yu, Y. P. Cai, C. Y. Su, X. M. Lin, X. X. Zhou, J. W. Cai, *Cryst. Growth Des.* **2008**, *8*, 4083 – 4091; c) H. S. Wang, B. Zhao, B. Zhai, W. Shi, P. Cheng, D. Z. Liao, S. P. Yan, *Cryst. Growth Des.* **2007**, *7*, 1851 – 1857; d) B. Zhao, H. L. Gao, X. Y. Chen, P. Cheng, W. Shi, D. Z. Liao, S. P. Yan, Z. H. Jiang, *Chem. Eur. J.* **2006**, *12*, 149 – 158; e) H. L. Gao, L. Yi, B. Zhao, X. Q. Zhao, P. Cheng, D. Z. Liao, S. P. Yan, *Inorg. Chem.* **2006**, *45*, 5980 – 5988; f) C. Qin, X. L. Wang, E. B. Wang, Z. M. Su, *Inorg. Chem.* **2005**, *44*, 7122 – 7129; g) B. Zhao, L. Yi, Y. Dai, X. Y. Chen, P. Cheng, W. Shi, D. Z. Liao, S. P. Yan, Z. H. Jiang, *Inorg. Chem.* **2005**, *44*, 911 – 920; h) B. Zhao, P. Cheng, X. Y. Chen, C. Cheng, W. Shi, D. Z. Liao, S. P. Yan, Z. H. Jiang, *J. Am. Chem. Soc.* **2004**, *126*, 3012 – 3013.

[15] a) H. L. Jiang, N. Tsumori, Q. Xu, *Inorg. Chem.* **2010**, *49*, 10001 – 10006; b) Y. G. Huang, F. L. Jiang, D. Q. Yuan, M. Y. Wu, Q. Gao, W. Wei, M. C. Hong, *J. Solid State Chem.* **2009**, *182*, 215 – 222; c) V. Chandrasekhar, B. M. Pandian, R. Boomishankar, A. Steiner, J. J. Viftal, A. Houri, R. Clerac, *Inorg. Chem.* **2008**, *47*, 4918 – 4929; d) L. P. Zhang, T. C. W. Mak, *Polyhedron* **2003**, *22*, 2787 – 2798; e) J. P. Costes, F. Dahan, F. Nicodeme, *Inorg. Chem.* **2003**, *42*, 6556 – 6563.

[16] a) P. Gawryszewska, Z. Ciunik, D. Kulesza, *J. Mol. Struct.* **2011**, *988*, 59 – 64; b) M. S. Tarasenko, N. G. Naumov, D. Y. Naumov, S. J. Kim, V. E. Fedorov, *Polyhedron* **2008**, *27*, 2357 – 2364; c) G. B. Deacon, C. M. Forsyth, *Chem. Eur. J.* **2004**, *10*, 1798 – 1840.

[17] Y. Q. Sun, J. Zhang, Z. F. Ju, G. Y. Yang, *Cryst. Growth Des.* **2005**, *5*, 1939 – 1943.

[18] a) S. Faulkner, S. J. A. Pope, *J. Am. Chem. Soc.* **2003**, *125*, 10526 – 10527; b) Z. Y. Du, H. B. Xu, J. G. Mao, *Inorg. Chem.* **2006**, *45*, 9780 – 9788.

[19] K. Aita, T. Temma, Y. Kuge, K. Seki, H. Saji, *Luminescence* **2010**, *25*, 19 – 24.

[20] a) D. P. Dong, L. Liu, Z. G. Sun, C. Q. Jiao, Z. M. Liu, C. Li, Y. Y. Zhu, K. Chen, C. L. Wang, *Cryst. Growth Des.* **2011**, *11*, 5346 – 5354; b) P. Wang, R.-Q. Fan, X.-R. Liu, L.-Y. Wang, Y.-L. Yang, W.-W. Cao, B. Yang, W. L. J. Hasi, Q. Su, Y. Mu, *CrystEngComm* **2013**, *15*, 1931 – 1949.

[21] a) X. Y. Chen, W. Zhao, R. E. Cook, G. K. Liu, *Phys. Rev. B* **2004**, *70*, 205122; b) X. Y. Chen, G. K. Liu, *J. Solid State Chem.* **2005**, *178*, 419 – 428; c) Z. H. Weng, D. C. Liu, Z. L. Chen, H. H. Zou, S. N. Qin, F. P. Liang, *Cryst. Growth Des.* **2009**, *9*, 4163 – 4170; d) H. B. Zhang, N. Li, C. B. Tian, T. F. Liu, F. L. Du, P. Lin, Z. H. Li, S. W. Du, *Cryst. Growth Des.* **2012**, *12*, 670 – 678.

[22] a) Z. J. Lin, L. W. Han, D. S. Wu, Y. B. Huang, R. Cao, *Cryst. Growth Des.* **2013**, *13*, 255 – 253; b) Y. Kataoka, D. Paul, H. Miyake, T. Yaita, E. Miyoshi, H. Mori, S. Tsukamoto, H. Tatewaki, S. Shinoda, H. Tsukube, *Chem. Eur. J.* **2008**, *14*, 5258 – 5266.

[23] N. Wartenberg, O. Raccurt, E. Bourgeat-Lami, D. Imbert, M. Mazzanti, *Chem. Eur. J.* **2013**, *19*, 3477 – 3482.

[24] C. B. Smith, C. L. Raston, A. N. Sobolev, *Green Chem.* **2005**, *7*, 650 – 654.

[25] Z. Wang, J. L. Yuan, K. Matsumoto, *Luminescence* **2005**, *20*, 347 – 351.

[26] E. S. Andreiadis, R. Demadrille, D. Imbert, J. Pcaut, M. Mazzanti, *Chem. Eur. J.* **2009**, *15*, 9458 – 9476.

[27] C. Galaup, J. M. Couchet, S. Bedel, P. Tisnés, C. Picard, *J. Org. Chem.* **2005**, *70*, 2274 – 2284.

[28] a) G. M. Sheldrick, SHELXS 97, Program for the Solution of Crystal Structures, Universität of Göttingen, Göttingen (Germany), **1997**; b) G. M. Sheldrick, SHELXTL-97, Program for the Refinement of Crystal Structures, Universität of Göttingen, Göttingen (Germany), **1997**.

Received: February 25, 2014

J. Xie, H.-M. Shu, H.-M. Hu,* Z.-X. Han, S.-S. Shen, F. Yuan, M.-L. Yang, F.-X. Dong, G.-L. Xue

■■ – ■■

Syntheses, Structures, and Luminescence Properties of Lanthanide Coordination Polymers with a Polycarboxylic Terpyridyl Derivative Ligand

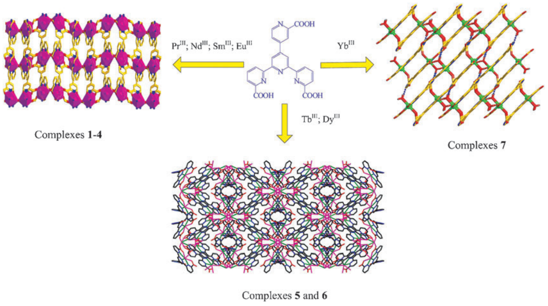

Made to fit: A new H_3L ligand, 4′-(3-carboxylpyridyl)-2,2′:6′,2″-terpyridine- 6,6″-dicarboxylic acid, is described for the formation of seven lanthanide–organic frameworks (see picture). The seven complexes crystallized in three structural types owing to the lanthanide contraction effect, which is reflected in the differences in the coordination number and geometry of lanthanide ions.